

Microscopic Characterizations of Few-Layer Hexagonal Boron Nitride: A Promising Analogue of Graphene

Application Note

Jing-jiang Yu, Shijie Wu, and Craig Wall
Agilent Technologies

Introduction

Graphene has generated dramatic interest recently due to its many unique properties,[1–3] and extensive research is being pursued on single- as well as few-layer graphene. One future direction in graphene-related research seeks alternative types of layered inorganic materials that act as analogues of graphene but also exhibit some needed attributes that graphene lacks.[4] In this context, hexagonal boron nitride (h-BN) is attracting considerable attention for two main reasons. First, hexagonal boron nitride is a layered material, similar to graphite. It is composed of sp^2 covalently bonded atoms in a honeycomb arrangement within each layer and therefore is iso-structural to graphene. As these layers are held together by weak van der Waals interactions, h-BN ultrathin films can be produced by mechanical exfoliation from a bulk crystal. Second, boron nitride is a wide band gap (more than 5 eV) III-V compound, whereas graphene is normally a zero-gap semiconductor. Current research predicts monolayer h-BN, a so-called “white graphene”, [5] is likely to be very useful as a complementary substrate for graphene electronics.

Originally micromechanical cleavage of HOPG was employed to obtain single-layer graphene. Despite recent advances, this mechanical

exfoliation method is still widely used for generating high-quality single-layer, as well as, few-layer graphene and its analogues. Several alternative synthetic routes have been developed. These routes include chemical vapor deposition (CVD) on the surface of a transition metal, such as Cu or Ni, and epitaxial growth on an insulator, such as SiC. Pioneering work on large-scale growth of atomic hexagonal boron nitride layers via a CVD process has been reported.[5] The ultimate goal is to generate extremely large, continuous, high-quality h-BN single- and few-layer films that are of similar quality to the ones prepared from micromechanical cleavage. However, there is still much room for improvement. In order to guide the optimization of the synthesis process, high-resolution surface characterization techniques are needed to provide detailed information regarding the qualities of as-grown h-BN films.

In this note, we report high-resolution microscopic characterizations of few-layer h-BN prepared from CVD, ranging from both qualitative observation and quantitative measurements of different layers within these ultrathin films. A variety of surface structures were observed by SEM and AFM, as well as comprehensive investigations of their local electric properties.



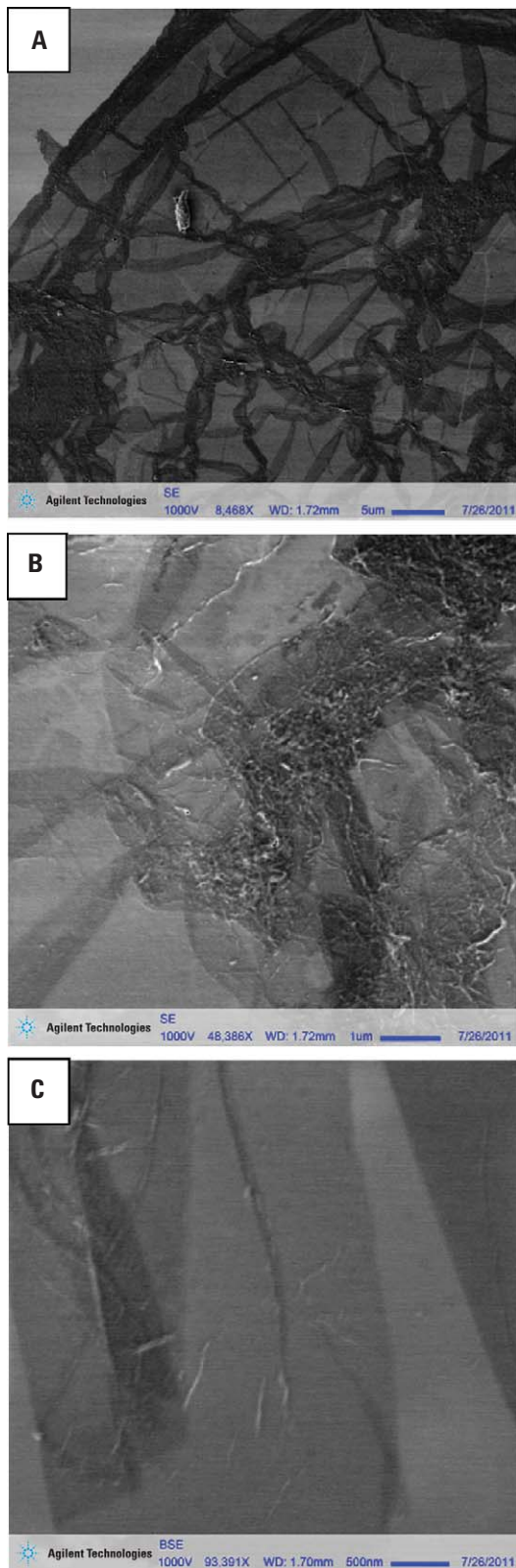


Figure 1. SEM secondary electron or backscattered electron images of h-BN layers synthesized via CVD on a silicon substrate. The corresponding scan sizes are (A) 50 μm , (B) 10 μm , and (C) 5 μm , respectively.

Qualitative thickness differentiation of few-layer h-BN ultrathin films via SEM imaging

As a high-throughput and ease-of-use characterization tool, the Agilent 8500 field emission scanning electron microscope (FE-SEM) is used for an initial examination of h-BN ultrathin films produced via CVD. Figure 1 presents three typical SEM images taken either from a large-scale view or small scale micrographs of selected locations corresponding to different surface features. Figure 1A is a secondary electron image with a large scan size of 50 $\mu\text{m} \times 50 \mu\text{m}$, in which the coexistence of both a bare, flat silicon substrate region exhibiting the brightest contrast at the upper-left corner and the remaining h-BN occupied area with a much darker contrast is clearly visible. Furthermore, two different types of surface features within the adsorbate-abundant region (i.e., the large and smooth areas that exhibit a gray color and some rougher locations with a much darker contrast) can be readily identified. Systematic zoom-in of selective locations containing these two features is carried out in subsequent SEM imaging. Figure 1B is another secondary electron image of a rough location with high magnification to provide a closer view, in which many entangled fibers are clearly observed. Figure 1C is a backscattered electron image with even higher magnification of a typical smooth area. SEM imaging at such scan size (5 $\mu\text{m} \times 5 \mu\text{m}$) effectively reveals the fine structural heterogeneity of the seemingly smooth and homogenous area. First, individual fibers and particles are captured. Second, successful differentiation of regions in that area is achieved unambiguously based on the intensity and contrasts that are resolved. From right to left, Figure 1C starts with a black (or the darkest) band, then a white (or the brightest) one, and then several gray levels (intensities) afterward.

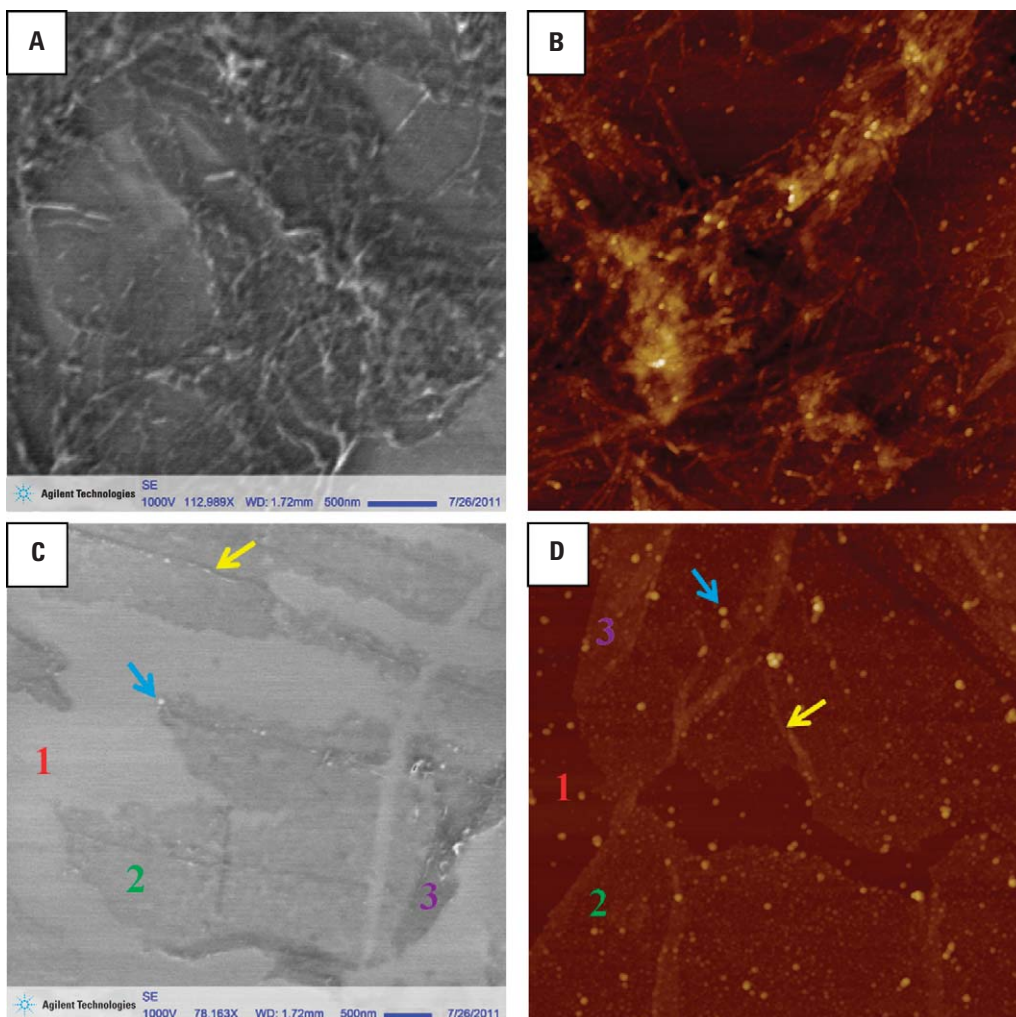


Figure 2. Correlation of SEM images with AFM data acquired from the same h-BN sample. (A) and (C) are representative SEM secondary electron images ($5\ \mu\text{m} \times 5\ \mu\text{m}$) of rough locations and smooth areas, respectively. (B) and (D) are typical AFM topographic images (with the identical size) of rough locations and smooth areas, respectively.

The same h-BN sample was also systematically characterized by AFM. One of the key capabilities of the AFM technique is offering 3-D (three-dimensional) and direct visualization of a sample's surface morphology with unprecedented spatial resolution. Figure 2 presents representative SEM secondary electron images of both rough locations and very smooth areas with corresponding AFM topographic images acquired with the same scan size. This side-by-side correlation of AFM and SEM data, though *ex situ*, renders further verification and a better understanding of the above-mentioned SEM images. Both techniques produce very consistent

results for the rough locations because similar entangled fibers are also captured by AFM (Figure 2A vs. Figure 2B). In the case of the very smooth areas, even more excitingly, a valid interpretation of the various contrasts in the SEM images is now possible with the help of the complementary AFM data. As illustrated by the colored numbers or symbols in Figures 2C and 2D, the white or brightest regions (indicated as red **1**) can be ascribed to the bare substrate while the lightest gray regions (green **2**) correspond to the thinnest films. Adsorbed h-BN films with increased layers or thickness will lead to a gradual darkening of their

contrasts. Therefore, the regions (purple **3**) with 2-D additional layers display a higher gray level. Other surface features, such as individual particles (blue arrows) and the nearly 1-D additional layers that are visible as elevated edges (yellow arrows), are captured in both the AFM and SEM images. Given the fact that few-layer h-BN ultrathin films prepared under these controlled synthesis conditions [5] are typically up to five layers (see Figure 3 and Figure 4), the capability for qualitative identification of various ultrathin h-BN films of different thickness (up to five layers) has been proven by these combined SEM and AFM studies.

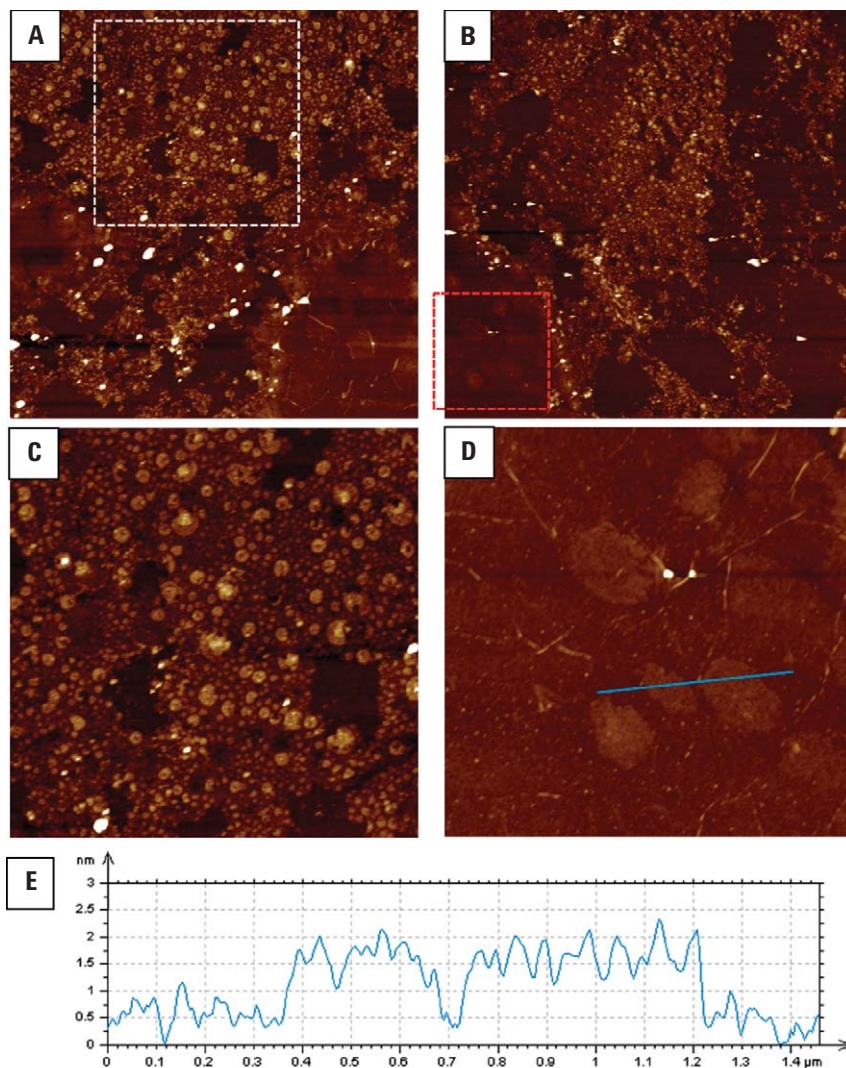


Figure 3. High-resolution AFM characterization of few-layer h-BN ultrathin films. (A) and (B) are two examples of topographic images revealing rich surface structures of few-layer h-BN ultrathin films. The scan size is $6\ \mu\text{m} \times 6\ \mu\text{m}$ and $10\ \mu\text{m} \times 10\ \mu\text{m}$, respectively. (C) is a zoom-in AFM topography ($3\ \mu\text{m} \times 3\ \mu\text{m}$) corresponding to the white square drawn in (A). (D) is a zoom-in AFM topography ($3\ \mu\text{m} \times 3\ \mu\text{m}$) corresponding to the red square drawn in (B). (E) is a cursor profile corresponding to the blue line drawn in (D).

Quantitative thickness measurements and high-resolution structural characterization of few-layer h-BN films using AFM

Regarding the possible growth pathway of hexagonal boron nitride on Cu foil during a CVD process, it is proposed that the copper substrate serves as a catalyst to accelerate the decomposition of ammonia borane ($\text{NH}_3\text{-BH}_3$) vapor at an elevated temperature, thus generating both boron and nitrogen atoms on the substrate. These chemical species may need to diffuse along the copper surface before they go through chemical reactions to form h-BN films. Therefore, this surface-mediated CVD process could be affected by

additional factors other than the delicate interplay between reaction kinetics and thermodynamics. For example, it is reported that the quality of the copper foil has a significant impact on both the formation of continuous layers on the substrate and the thickness (number of layers) of the resultant h-BN films.[5]

Figures 3A ($6\ \mu\text{m} \times 6\ \mu\text{m}$) and 3B ($10\ \mu\text{m} \times 10\ \mu\text{m}$) are two topographic images that are representative of the quality of a specific h-BN sample. First, defect areas such as patches of unoccupied substrate inlaid within the h-BN film are easily resolved at this scan size, implying that it is still challenging to routinely achieve

perfectly continuous h-BN layers at tens-of-micrometers length scales. In addition, the surface exhibits structural heterogeneity. Figure 3C provides a zoom-in topographic image of a rough location indicated by a white square in Figure 3A. Adversely affecting the overall sample quality, many particles are observed on top of the h-BN film and can probably be attributed to some residual precursors. However, some regions corresponding to high-quality h-BN films are observed. Figure 3D is the zoom-in of one such location, indicated by a red square in Figure 3B. Its surface morphology is both smooth and very uniform; its quality is close to that of films produced

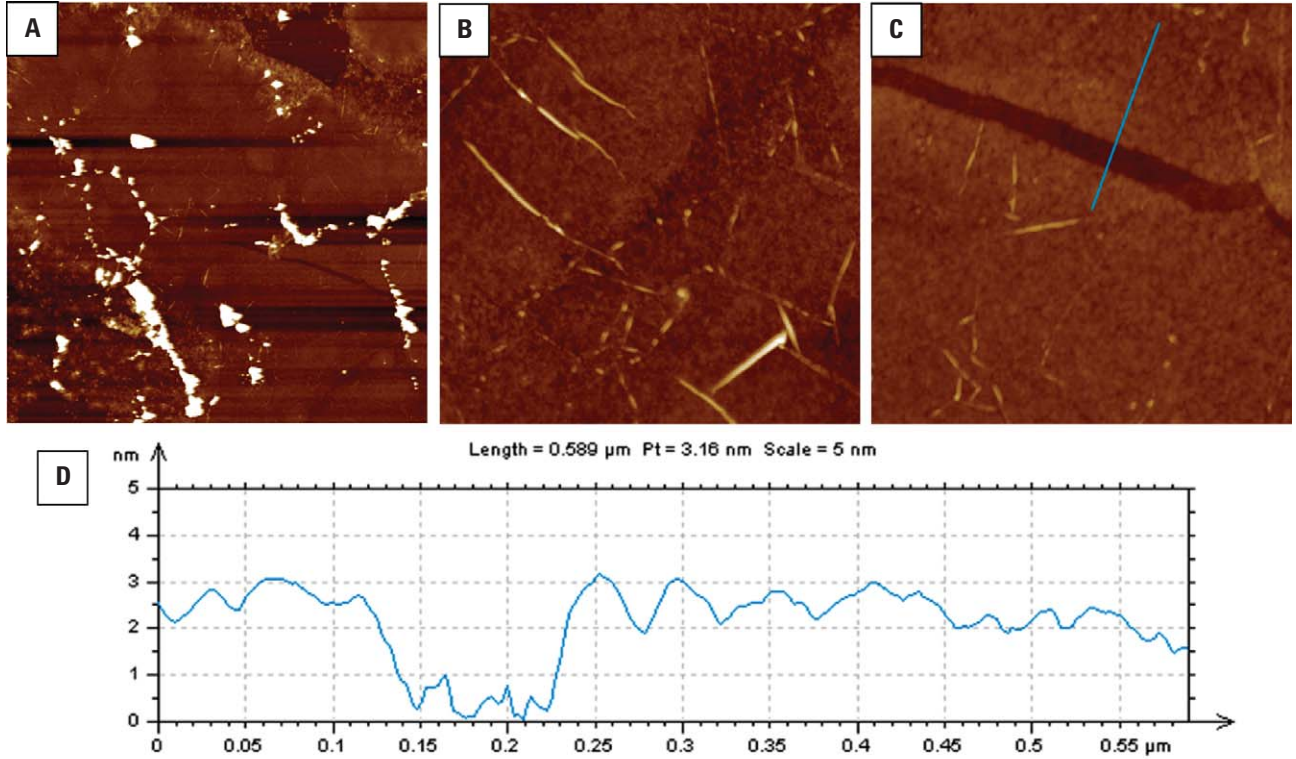


Figure 4. An example of large-scale growth of high-quality h-BN films with thickness measurements. (A) is an $8\ \mu\text{m} \times 8\ \mu\text{m}$ AFM topographic image showing large-scale production of high-quality h-BN films. (B) and (C) are two examples of zoom-in AFM topographies ($1.5\ \mu\text{m} \times 1.5\ \mu\text{m}$) of the high-quality areas. (D) is a cursor profile corresponding to the blue line drawn in (C).

using the mechanical exfoliation method. Several islands are shown in this image. Figure 3E is the line profile corresponding to the blue line drawn in Figure 3D that spans two of the islands. The apparent height of these islands is about 1 nm, which is in good agreement with the thickness of a single atomic h-BN layer. Also captured in Figure 3D are a few wrinkles, which were likely introduced by the transfer process or induced by the grain boundaries on the underlying substrate.

Figure 4A is a topographic image ($8\ \mu\text{m} \times 8\ \mu\text{m}$) acquired at a particular location on the same sample.

A super-sized region (more than $10\ \mu\text{m}$ along its long-axis direction) of high-quality h-BN film has been observed. High-resolution imaging at higher magnification clearly reveals a boundary in Figure 4B and a long trench in Figure 4C. This trench allows the absolute thickness of h-BN films in this region to be quantified easily. Figure 4D is the line profile corresponding to the blue line in Figure 4C, from which we can see that the depth of the trench is about 2 nm. Combined with the thickness measurement in Figure 3, we can conclude that most of the h-BN film within this region is two layers and the islands are three layers.

Probing local electric properties of few-layer h-BN ultrathin films using AFM

Several advanced imaging modes of AFM are used to characterize local electric properties of few-layer h-BN films. Figure 5 presents electric force microscopy (EFM) studies of few-layer h-BN and correspondingly similar graphene films on silicon substrates. Both materials were measured by the same tip under identical imaging conditions for a side-by-side comparison, capturing their very different impacts on the electric force tip-sample interactions. The h-BN films show a similar response with respect to silicon, since there is negligible contrast variation in the EFM image (Figure 5B); graphene has a stronger response than the substrate material on the tip sample interaction, as a much brighter contrast corresponding to the graphene location is shown in the EFM image (Figure 5D).

The conductivity of h-BN ultrathin films is examined by a current-sensing AFM (CS-AFM), also known as conductive AFM. Figure 6A shows the surface morphology of an excellent few-layer h-BN sample prepared on a conductive substrate HOPG. This h-BN film is extremely uniform and continuous; no defects or holes exposing HOPG underneath are captured. Therefore, a desired HOPG

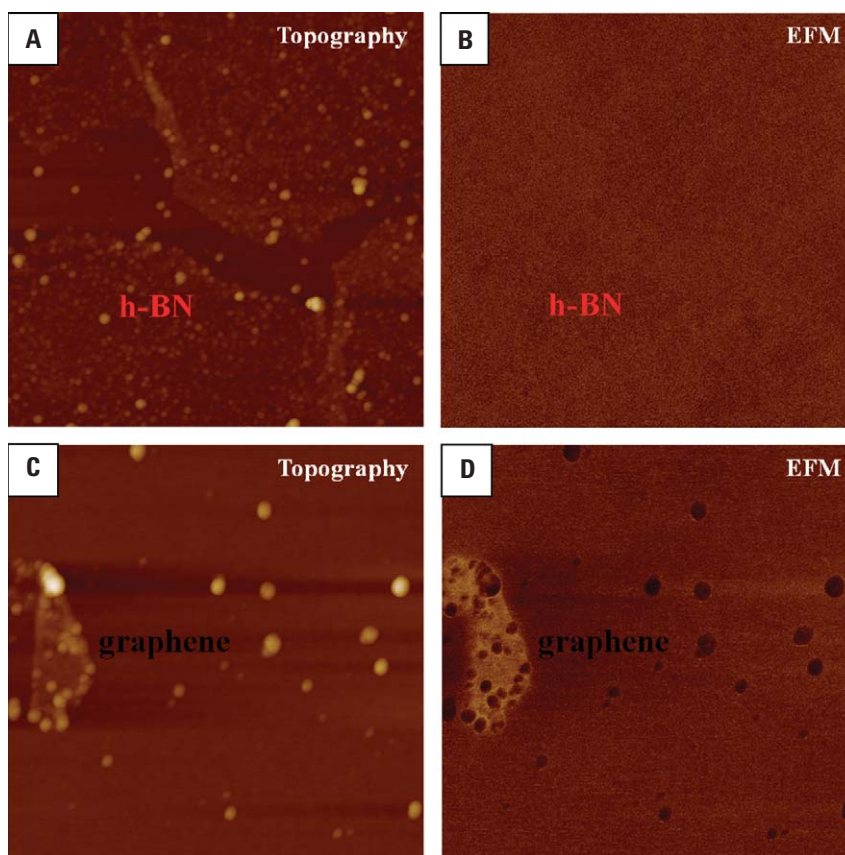


Figure 5. EFM studies of few-layer h-BN and graphene on silicon. (A) and (B) are a topographic image and a corresponding EFM image of a few-layer h-BN film on silicon, respectively. Scan size: $3\mu\text{m} \times 3\mu\text{m}$. (C) and (D) are a topographic image and a corresponding EFM image of a few-layer h-BN graphene film on silicon, respectively. Scan size: $2\mu\text{m} \times 2\mu\text{m}$.

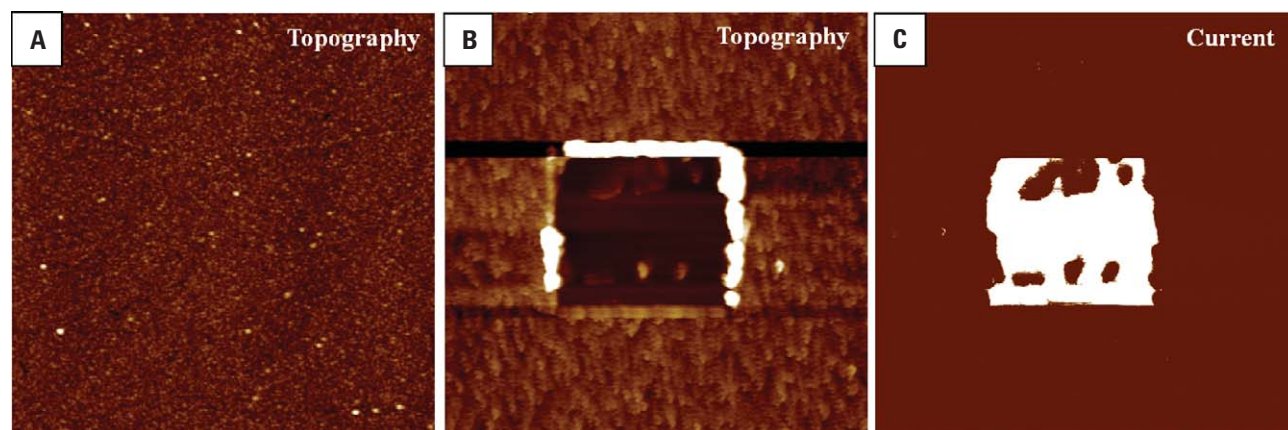


Figure 6. CS-AFM studies of few-layer h-BN on HOPG. (A) is a topographic image showing uniform and continuous h-BN layers on HOPG. Scan size: $10\mu\text{m} \times 10\mu\text{m}$. (B) and (C) are a topographic image and a corresponding current image, respectively, after a pattern area of exposed HOPG has been produced by AFM-based lithography. Scan size: $5\mu\text{m} \times 5\mu\text{m}$.

area mimicking the graphene (single-layered graphite) is fabricated using an AFM-based lithography method by which the h-BN film is displaced locally by an AFM tip in contact mode with a high force. The resultant surface after local abrasion is shown in Figure 6B, in which a $2\ \mu\text{m} \times 2\ \mu\text{m}$ HOPG pattern is produced with aggregates of displaced h-BN film around the edges and at a few locations within the pattern area (a typical phenomenon associated with this AFM-based mechanical scratching). Figure 6C is the corresponding current image. Only the unoccupied HOPG areas exhibit a detectable current signal, implying that h-BN is insulating while graphene is conductive.

Such h-BN vs. graphene results from both CS-AFM and EFM studies are well expected and might be attributable to the intrinsic difference between the two materials at the molecular level. Monolayer hexagonal boron nitride is isoelectronic (having the same number of electrons) with respect to graphene; all of the atoms (the boron and nitrogen in h-BN films and the carbon in graphene) adopt an sp^2 hybridization. Therefore, h-BN films, compared to graphite, are lacking the conjugated pi electrons that are delocalized and more mobile. As a result, weaker electric force interactions (with an AFM tip applied with an AC voltage) and a lower conductivity is detected in the case of the few-layer h-BN materials in our AFM investigations.

A recently developed AFM technique known as scanning microwave microscopy (SMM) was utilized to provide complementary information to the CS-AFM and EFM results. It consists of an atomic force microscope interfaced with a vector network analyzer (VNA). In reflection mode (S11 measurement), the measured complex reflection coefficient of the microwave from the contact point directly correlates to the impedance of the sample under test. Since the measured load impedance is largely determined by the impedance of the

sample under test, SMM can be used to measure the capacitances over dielectric thin films and consequently to study the dielectric properties of the thin film material. Details about both the principles and instrumentation of SMM can be found in other application notes from Agilent (F.M. Serry, Scanning Microwave Microscope, Agilent application note 5989-8818EN; W. Han, Introduction to Scanning Microwave Microscopy, Agilent application note 5989-8881EN).

SMM results for few-layer h-BN films are shown in Figure 7. The topography image (Figure 7A) shows that the structure of the h-BN film under study is similar to that revealed by high-resolution AFM imaging (Figure 4D), including both a smooth and continuous background of double-layer films and a few three-layer islands. The capacitance images (PNA amplitude and PNA phase shown in Figures 7B and 7C, respectively) acquired at the same time reveal that the double-

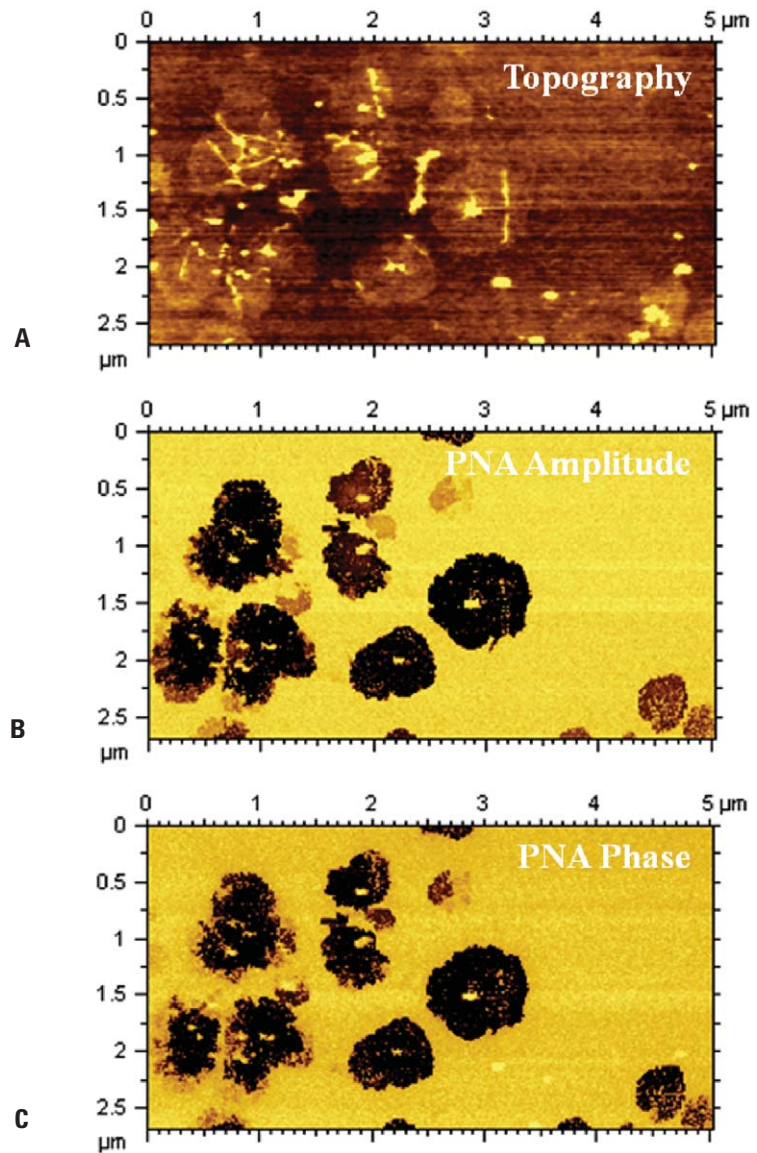


Figure 7. SMM studies of few-layer h-BN on silicon. (A) is a topographic image of a high-quality few-layer h-BN film. (B) and (C) are the corresponding PNA amplitude and PNA phase images, respectively. Scan size: $5\ \mu\text{m} \times 2.75\ \mu\text{m}$.

layer films are fairly uniform across the region. Even though wrinkles caused by the material transfer process or grain boundaries of the underlying substrate are resolved in the topographic image, they do not contribute to the capacitance images. This indicates that capacitance images are dominated by the film thickness and the dielectric properties of the film. It is interesting, however, to see that the contrast variation (likely the capacitance difference) between the three-layer islands and the surrounding double-layer region is clearly differentiated in Figures 7B and 7C. Since the difference in thickness between the layers is only about 1 nm and the overall film thickness is about 3 nm, the contribution of the film thickness to the observed capacitance difference is small. Therefore, the observed capacitance difference has to do with possible changes in the local dielectrics of the three-layer film. As previously mentioned, the formation of three-layer islands could be due to local defects on the substrate, which in turn could affect the capacitance measured by SMM. A better understanding of the measured capacitance difference may require additional knowledge of both the structures and local electronic properties of the h-BN film as well as that of the substrate. Further SMM investigation of h-BN ultrathin films will be carried out in the near future.

Summary

Few-layer hexagonal boron nitride films prepared from a chemical vapor deposition process have been systematically studied from a microscopic point of view. SEM imaging shows its qualitative capability of resolving various thickness or number of layers of these ultrathin films (up to five layers). AFM can provide both quantitative measurements of film thickness and high-resolution structural characterization, such as resolving the rich and fine structures or domains within the film. In addition, the local electric properties of h-BN films are measured with various advanced AFM imaging modes and prove to be dramatically different from those of graphene.

Acknowledgment

The authors thank Dr. Zheng Liu and Prof. Pulickel M. Ajayan at Rice University for all of the h-BN and graphene samples received for this application note as well as for many helpful discussions.

References

1. Geim *et al.* *Nat. Mater.* **2007**, *10*, 183-191.
2. Geim *et al.* *Science* **2009**, *324*, 1530-1534.
3. Rao *et al.* *Angew. Chem. Int. Ed.* **2009**, *48*, 7752-7777.
4. Rao *et al.* *J. Phys. Chem. Lett.* **2010**, *1*, 572-580.
5. Song *et al.* *Nano Lett.* **2010**, *10*, 3209-3215.

Nanomeasurement Systems from Agilent Technologies

Agilent Technologies, the premier measurement company, offers high precision instruments for nanoscience research in academia and industry. Exceptional worldwide support is provided by experienced application scientists and technical service personnel. Agilent's leading-edge R&D laboratories ensure the continued, timely introduction and optimization of innovative, easy-to-use nanomeasurement system technologies.

www.agilent.com/find/nano

Americas

Canada	(877) 894 4414
Latin America	305 269 7500
United States	(800) 829 4444

Asia Pacific

Australia	1 800 629 485
China	800 810 0189
Hong Kong	800 938 693
India	1 800 112 929
Japan	0120 (421) 345
Korea	080 769 0800
Malaysia	1 800 888 848
Singapore	1 800 375 8100
Taiwan	0800 047 866
Thailand	1 800 226 008

Europe & Middle East

Austria	43 (0) 1 360 277 1571
Belgium	32 (0) 2 404 93 40
Denmark	45 70 13 15 15
Finland	358 (0) 10 855 2100
France	0825 010 700* *0.125 €/minute
Germany	49 (0) 7031 464 6333
Ireland	1890 924 204
Israel	972-3-9288-504/544
Italy	39 02 92 60 8484
Netherlands	31 (0) 20 547 2111
Spain	34 (91) 631 3300
Sweden	0200-88 22 55
Switzerland	0800 80 53 53
United Kingdom	44 (0) 118 9276201

Other European Countries:

www.agilent.com/find/contactus

Product specifications and descriptions in this document subject to change without notice.

© Agilent Technologies, Inc. 2011
Printed in USA, August 16, 2011
5990-8893EN



Agilent Technologies